

03,08

## Adsorption of potassium atoms on the surface of AlN(0001)

© M.N. Lapushkin

Ioffe Institute,  
St. Petersburg, Russia  
E-mail: lapushkin@ms.ioffe.ru

Received April 30, 2025

Revised July 7, 2025

Accepted July 9, 2025

The adsorption of potassium atoms on the AlN(0001) surface was calculated by the density functional method. The 2D AlN layer was modeled by the AlN(0001)  $2 \times 2 \times 2$  supercell containing 10 AlN bilayers. It was shown that adsorption of K atoms in the hollow position and over surface N atoms is preferable at a coverage of 0.25 monolayer, and the adsorption energies of K atoms are  $-1.51$  eV and  $-1.53$  eV, respectively. At a monolayer coverage, adsorption of K atoms is preferable over surface N atoms, and the adsorption energy of K atoms is  $-0.93$  eV. It was shown that adsorption of potassium atoms leads to the formation of surface states, the electron density of which is localized near the Fermi level.

**Keywords:** AlN, potassium, adsorption, electronic structure.

DOI: 10.61011/PSS.2025.07.61868.100-25

### 1. Introduction

Devices created using metal trinitrides are becoming increasingly widespread in the 21st century in various fields of electronics. GaN-based devices retain the leading role. Other metal trinitrides are also not ignored by scientists and manufacturers of electronic devices. AlN has high thermal stability, good high-frequency energy characteristics and a large band gap [1] than GaN, which ensures its use in the creation of devices that operate in the ultraviolet range (UV). AlN-based devices allow the creation of UV-emitting photodiodes, sun-blind light detectors, optomechanical devices, etc. [1–6]. A promising direction is the use of hollow AlN nanoparticles decorated with lithium to store hydrogen [7,8]. It is possible to create batteries without using lithium [9].

The adsorption of alkali metals on the surface changes the electronic structure of the surface, which changes its physico-chemical properties. However, calculations of the adsorption of alkali metal atoms on the surface of AlN are many times less than calculations of the adsorption of alkali metal atoms on the surface of GaN [10]. The adsorption of alkali metal atoms on the AlN surface was calculated only for Li, Na, and Cs. The adsorption of submonolayer coatings of Cs atoms on the surface of AlN(0001) doped with Si atom is calculated in Ref. [11]. The 2D layer AlN(0001) consisted of 6 AlN bilayers. It is shown that the adsorption energy ( $E_{\text{ads}}$ ) of caesium atoms decreases with an increase in the cesium coverage from  $-1.5$  eV to  $-0.5$  eV with an increase in the coverages from 0.25 monolayer (ML) to 1.0 ML, respectively. The preferred place of adsorption of Cs atoms with a coverage of 0.25 ML is the position above the N atom. The adsorption of caesium atoms leads to a slight downward shift of the electronic states, which indicates a downward bending of

the zones. The adsorption of lithium atoms and ions on the surface of a hexagonal monolayer and a zigzag nanotube AlN was calculated in Ref. [8]. The adsorption energy of lithium atoms is insignificant and is equal to  $-0.32$  eV and  $-0.05$  eV on a nanotube and an AlN monolayer, respectively. The adsorption of lithium ions turns out to be energetically advantageous compared to the adsorption of Li atoms, since  $E_{\text{ads}}$  is equal to  $-1.22$  eV and  $-1.16$  eV on a nanotube and an AlN monolayer, respectively. The adsorption of Li and Na atoms on a hexagonal monolayer  $3 \times 3$  supercell of AlN has been calculated in Ref. [12]. The adsorption energy in the dimpled position was equal to  $-1.51$  eV and  $-0.83$  eV for Li and Na, respectively. Calculations have shown that the 2D AlN layer can be used as an anode in lithium-ion and sodium-ion batteries with a theoretical capacity of 500 and  $385 \text{ mA} \cdot \text{h} \cdot \text{g}^{-1}$ , respectively. The adsorption of lithium atoms and ions on the surface of AlN nanotubes of various diameters has been calculated in Ref. [13] in order to simulate lithium-ion batteries. It has been shown that lithium adsorption on the surface of nanotubes is preferable, and the adsorption energy decreases with increasing nanotube diameter. The adsorption energy of the Li atom is of the order of  $\sim 0.6$  eV, the adsorption energy of the Li ion is  $-1.7$  eV. The adsorption of a sodium atom on the surface of a monolayer hexagonal  $5 \times 5$  supercell of AlN has been calculated in Ref. [13]. The adsorption energy of the Na atom is of the order of  $-0.16$  eV. The adsorption energy of the Na ion turned out to be  $-1.65$  eV. The adsorption of a lithium atom on a hexagonal (h) monolayer of AlN and GaN is calculated in Ref. [14]. It was found that lithium adsorption is preferred in the dimpled position and the energy of Li adsorption on h-AlN reaches the value of  $-1.241$  eV, and the energy of lithium adsorption on h-GaN turned out to be equal to  $-1.684$  eV. It is shown that the adsorption energy

of lithium on h-AlN is equal to  $-0.938\text{ eV}$  and  $-0.885\text{ eV}$  for adsorption over the Al and N atom, respectively.

The adsorption of a lithium atom on a hexagonal monolayer of AlN is also calculated in Ref. [8]. It was found that lithium adsorption on h-AlN is preferred in the dimpled position and  $E_{\text{ads}} = -1.27\text{ eV}$ . Lithium-doped AlN surfaces increase the binding energy of the hydrogen molecule from  $0.14\text{ eV}$  to  $0.20\text{ V}$ . The system demonstrates a high theoretical molecular hydrogen storage capacity of  $8.25\text{ wt.\%}$ . The molecular storage capacity of hydrogen on the surface of hollow AlN nanoparticles decorated with lithium atoms was studied in Ref. [15]. It is shown that the binding energy of the hydrogen molecule decreases with the size of the nanoparticle and lithium decoration of the surface of the hollow nanoparticle increases the binding energy of the hydrogen molecule, which leads to an increase in the molecular capacity from  $4.7\text{ wt.\%}$  to  $9\text{ wt.\%}$ . The diffusion of Li, Na, and K atoms over the surface of a nanocage  $(\text{AlN})_{12}$  was calculated in Ref. [15].

Little attention has been paid to the study of potassium adsorption on AlN. The adsorption of sublayer potassium coatings on the AlN surface was studied using photoelectron spectroscopy in Refs. [16,17]. Changes in the spectra of the valence band and core levels of  $\text{Al}2p$ ,  $\text{N}1s$  and  $\text{K}3p$  were recorded. For a pure AlN surface, the spectrum of the valence band represents a wide peak without features with a maximum of  $4\text{ eV}$  below the maximum of the valence band ( $E_{\text{VBM}}$ ). A peak of surface states was identified, located at  $E_{\text{VBM}}$ . The adsorption of  $0.9\text{ ML}$  of potassium leads to suppression of the peak of surface states and a change in the spectrum of the valence band in the region of high binding energies with a maximum at  $6.6\text{ eV}$  below  $E_{\text{VBM}}$ , which the authors of the article in Refs. [16,17] explained by the formation of induced surface states.

Obviously, little attention has been paid to calculations of the adsorption of alkali metal atoms on various AlN surfaces, and they consider only the adsorption of lithium, sodium, and caesium atoms on various nanostructures: from a 2D AlN layer, including a monolayer hexagonal AlN supercell, to nanotubes and hollow AlN nanoparticles. There are still no calculations of the adsorption of potassium atoms on the surface of AlN(0001), which would make it possible to understand the results of an experimental study of this adsorption system. Therefore, the task was set to calculate the electronic structure of the 2D layer of AlN(0001) in the valence band region and show how potassium adsorption affects the electronic structure of the 2D layer of AlN(0001).

## 2. Calculation details

First-principle calculations are performed within the framework of the DFT density functional theory implemented in the QUANTUM ESPRESSO package [18] using the exchange-correlation functional described in the local density approximation (LDA —local density approximation)

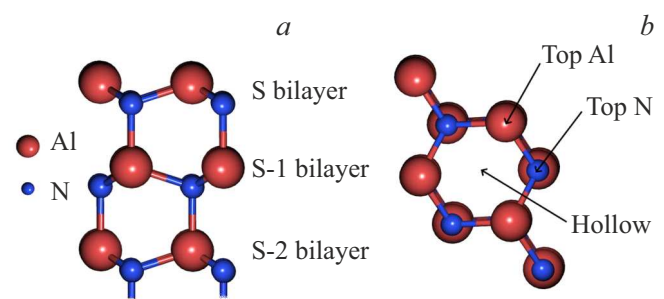


**Figure 1.** *a)* 2D layer AlN(0001): side view, showing only the top three bilayers of AlN. The letter S indicates the surface bilayer AlN. The layers are numbered from the surface bilayer AlN. *b)* Adsorption sites of K adatoms on the 2D AlN layer: top view. Red ball — atom Al, blue ball — atom N. The arrows show the adsorption sites of K atoms.

in the form of Perdew-Zunger (PZ) interpolation [19]. The 2D AlN layer was modeled by a supercell (0001)  $2 \times 2 \times 2$ . The vacuum gap between the 2D layers was  $18\text{ \AA}$  to avoid the influence of parasitic electric fields. Kinetic energy limit and charge density limit were set to  $40\text{ Ry}$  and  $350\text{ Ry}$ . A gamma-centered grid with  $k$ -points  $4 \times 4 \times 1$  is used for all 2D systems in this article.

AlN has a wurtzite structure with the following lattice parameters:  $a = b = 3.219\text{ \AA}$  and  $c = 5.017\text{ \AA}$ . Two cases of adsorption were considered: in the first case, one K atom accounts for 4 surface atoms of Al, and in the second case, 4 potassium atoms account for 4 surface atoms of Al, which corresponds to one monolayer (ML) of potassium atoms. The supercell consists of 10 AlN bilayers (Figure 1). Only 3 upper bilayers of AlN were subjected to relaxation. The position of the remaining AlN bilayers was fixed, which was done to simulate the volume of AlN. The nitrogen atom bonds of the GaN lower bilayer were saturated with pseudo hydrogen atoms. Relaxation of the supercell parameters was performed until the moduli of the forces were smaller than  $10^{-7}\text{ Ry/Bohr}$ .

## 3. Results and discussion

Relaxation of the 2D layer of AlN(0001) without adsorbate leads to relaxation of the surface layers relative to the unrelaxed 2D layer of AlN(0001). The amount of relaxation can be determined from the following equation:  $4s$  where

$$\Delta_{ij} = (d_{ij} - d_{0ij})/d_{0ij} \quad (1)$$

is the relative change in the distance between the  $\Delta_{ij}$ -th and  $i$ -th layers of Al atoms for a relaxed and non-relaxed 2D layer.  $j$  is the distance between  $\Delta_{ij}$  and  $i$  layer of Al atoms for an unrelaxed 2D layer and  $d_{0i}$  is the distance between the  $\Delta_{ij}$ -th and  $i$ -th layer of Al atoms for a relaxed 2D layer. The „-“ sign indicates a decrease in distance. The found value of  $\Delta_{12}$  is too small ( $\Delta_{12} = -0.00095$ ),

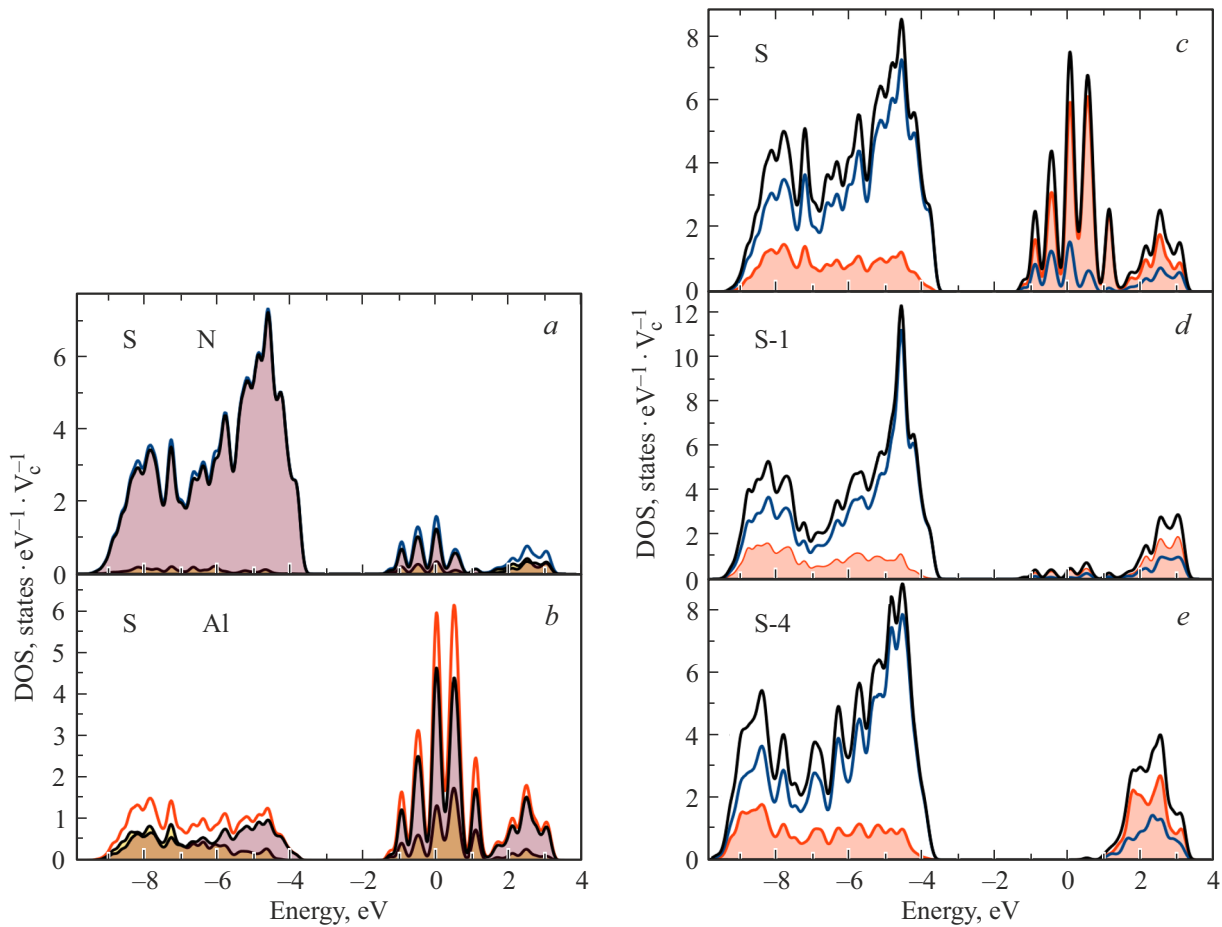


**Figure 2.** Calculated total and partial densities of states of the 2D layer AlN(0001). Partial densities of states N (a) and Al (b) for the surface S bilayer AlN. Total and partial densities of states for S (c), S-1 (d) and S-4 (e) bilayers AlN.  $V_c$  — unit cell volume. Total density of states: AlN — black color, N — blue color. Partial densities of states: N 2s — yellow with fill, N 2p — pink with fill, Al — red, Al 3p — pink fill and Al 3s — yellow fill.

which indicates almost the same interlayer distances as in the nonrelaxed part of the 2D layer.

The adsorption energy  $E_{\text{ads}}$  of K atoms on the AlN surface can be calculated from the following equation:  $\Delta_{12} = -0.00095$  where

$$E_{\text{ads}} = (E_{\text{K/AlN}} - E_{\text{AlN}} - n \cdot E_{\text{K}})/n \quad (2)$$

and  $E_{\text{K/AlN}}$  are total surface energies with and without adsorbed K,  $E_{\text{AlN}}$  is the total atomic energy K,  $E_{\text{K}}$  is the quantity of K atoms in a unit cell (1 or 4).

The values of the adsorption energy of K atoms in three positions: hollow, above the surface atom Al (top Al) and above the surface atom N (top N), as well as the distances between the plane formed by the centers of the surface atoms Al(N) and the position of the adsorbed atom K, are shown in the table. The obtained values of the adsorption energy of potassium atoms are close to the values of the adsorption energy of other alkali metal atoms [11,12].

When 0.25 ML of potassium atoms are adsorbed, the difference between the adsorption energies at the hollow and top N positions is insignificant, and in both cases

The adsorption energy of the potassium atom and the distance (h) between the level of surface atoms Al and the plane of adsorbed atoms K

Coverage	0.25 ML		1.0 ML	
	$E_{\text{ads}}$ , eV	h, Å	$E_{\text{ads}}$ , eV	h, Å
hollow	-1.51	3.11	—	—
top Al	-1.42	3.08	-0.77	3.53
top N	-1.53	3.08	-0.93	3.09

a K atom forms a bond with three aluminum atoms. The adsorption of a monolayer of potassium atoms is preferable over N atoms. The results of other calculations [11–14] shows that the preferred sites of adsorption are top N or in the hollow position, which depends on the type of AlN structure chosen by the authors of the papers. The decrease in the adsorption energy with increasing coating coincides with the results of calculations of the adsorption of Cs atoms on the surface of AlN(0001) doped with the atom Si [11].

The AlN surface does not undergo surface reconstruction caused by the adsorption of 0.25 ML of potassium atoms. The value of the relaxation value „—“ of the surface has the same value as for the pure surface AlN.

The adsorption of 1.0 ML of potassium atoms leads to a small reconstruction of the AlN surface, which is caused by the interaction of valence electrons of the adsorption system. The surface atoms of AlN (S bilayer) are shifted upward relative to the case of adsorption of 0.25 ML of potassium atoms, and the following value is obtained for the relaxation value of the surface:  $n$ .

Figure 2 shows the calculation of the electron density of states (DOS is the density of states) of the 2D layer AlN(0001). A zone of occupied surface states is observed for the surface bilayer (S) with maxima at energies  $-0.89$  eV,  $-0.44$  eV and  $0.05$  eV. The zone is formed by Al 3s, Al 3p and N 2p-states with a predominance of Al states (Figure 2, *a*—*c*). The presence of a zone of occupied surface conditions indicates the metallization of the surface. There is also a pseudo-gap between the maximum of the valence band and the bottom of the zone of surface states with a width of  $1.9$  eV. The electron density of surface states sharply drops for the S-1 bilayer below the Fermi level, which indicates the spatial localization of surface states (Figure 2, *d*). The wide valence band is formed mainly by N 2p-states with a significantly lower contribution of Al 3s and Al 3p-states, has two peaks at a  $-4.50$  eV and  $-7.50$  eV (Figure 2, *e*) and corresponds to the electronic structure of an AlN crystal with a band gap of  $3.76$  eV.

The valence band of the 2D layer AlN(0001) with two maxima was obtained in Ref. [11], and two maxima in the valence band can also be distinguished for *h*-AlN [15]. The semiconductor character of AlN was obtained in Refs. [11,15] when calculating *h*-AlN. An analysis of the literature has shown that few spectra of the valence band of AlN have been obtained using photoelectron spectroscopy. The spectra of the valence band under excitation by a helium lamp are shown in Ref. [20]. A maximum can be identified at  $h\nu = 40.8$  eV for  $-7.50$  eV in this spectrum and a singularity at  $-5$  eV and a feature at  $-9$  eV. In Refs. [16,17], a single peak was observed with a maximum of  $4$  eV below  $E_{VBM}$ . The surface layer and the layers closest to it are probed at a given excitation energy. At high excitation energies  $h\nu = 1486.6$  eV and  $1253.6$  eV, at which electron photoemission occurs from the depth of the sample, the presence of two peaks in the valence band below  $E_{VBM}$   $-6.0$  eV and  $-1.9$  eV is shown [21]. These values are close to the position of the maxima in the valence band for the S-4 bilayer (below  $E_{VBM}$  by  $-5.0$  eV and  $-1.4$  eV).

The difference between the calculation and the experimental data may be due to the fact that the actual topography and stoichiometry of the AlN surface differs from the ideal one for which the present calculation was made. The presence of various surface defects on a real surface can have an impact on the experimental data obtained.

The results of calculating the electronic structure of the K/AlN(0001) system with a coating of 0.25 potassium and a monolayer during adsorption of K over N atoms are shown in Figure 3. Figure 3, *a* shows the zone of surface states of potassium, which is formed by 4s- and 4p-states. Three peaks are visible in the area below the Fermi level:  $-1.10$  eV,  $-0.73$  eV and  $-0.10$  eV. The pseudogap width in the S bilayer decreases from  $1.90$  eV for a pure AlN surface to  $1.22$  eV after potassium adsorption.

The adsorption bond is formed due to the interaction of potassium valence electrons with unpaired electrons of dangling Al bonds. This interaction leads to a significant change in the electronic structure of the surface bilayer and smaller changes in the S-1 bilayer, as shown in Figure 3, *b*—*e*. The effect of adsorbed potassium becomes insignificant already for the S-4 bilayer (Figure 3, *f*). In the region of the surface states of AlN, there is a shift towards lower energies up to  $0.25$  eV: the maxima are located at  $-1.14$  eV,  $-0.70$  eV and  $-0.05$  eV. The area of unoccupied states varies slightly. The valence band is also undergoing changes: it is shifting towards higher energies by  $0.4$  eV. A shift of surface states below the Fermi level towards lower energies up to  $0.40$  eV also takes place in the S-1 bilayer. The change in the area of unoccupied states is also insignificant. The valence band shifts towards higher energies by  $0.4$  eV. Accordingly, the pseudo-gap decreases to a value of  $1.27$  eV. The changes in the electronic structure of the S-4 bilayer are small: a shift of the valence band towards high energies by  $0.18$  eV and the band gap becomes  $3.64$  eV.

Even the adsorption of 4 times fewer lithium atoms [15], than in the present calculation, leads to a change in the valence band *h*-AlN: many maxima appear in it. A 2D layer consisting of 10 AlN bilayers is calculated in this paper, while only one hexagonal AlN monolayer is considered in Ref. [15], which leads to different results. Obviously, the effect of adsorbate on the substrate is greater for thinner substrates than for thick substrates. As in the present work, the peak of the adsorbate of lithium states at the Fermi level was found in Ref. [15]. It is shown in Ref. [11] that the adsorption of Li and Na atoms on the surface of AlN leads to the formation of an adsorbate surface zone at the Fermi level. In the present calculation, the zone of surface states is located at the Fermi level, which indicates the metallization of the surface and this zone is located at an energy higher than  $E_{VBM}$ , which differs from the results provided in Refs. [16,17].

Figure 4, *a* shows the difference in charge density  $\Delta\rho(r)$  after potassium adsorption at a position above the nitrogen atom, which is calculated from the equation:

$$\Delta\rho(r) = (\rho_{K/AlN}(r) - \rho_{AlN}(r) - \rho_K(r)) \quad (3),$$

where the charge density  $\rho_{K/AlN}(r)$  for the K/AlN(0001) layer,  $\rho_{AlN}(r)$  for the AlN(0001) layer and  $\rho_K(r)$  for the K layer. The charge accumulates under the potassium atom and the charge leaves the area of the potassium atom, which indicates the formation of a bond between the potassium

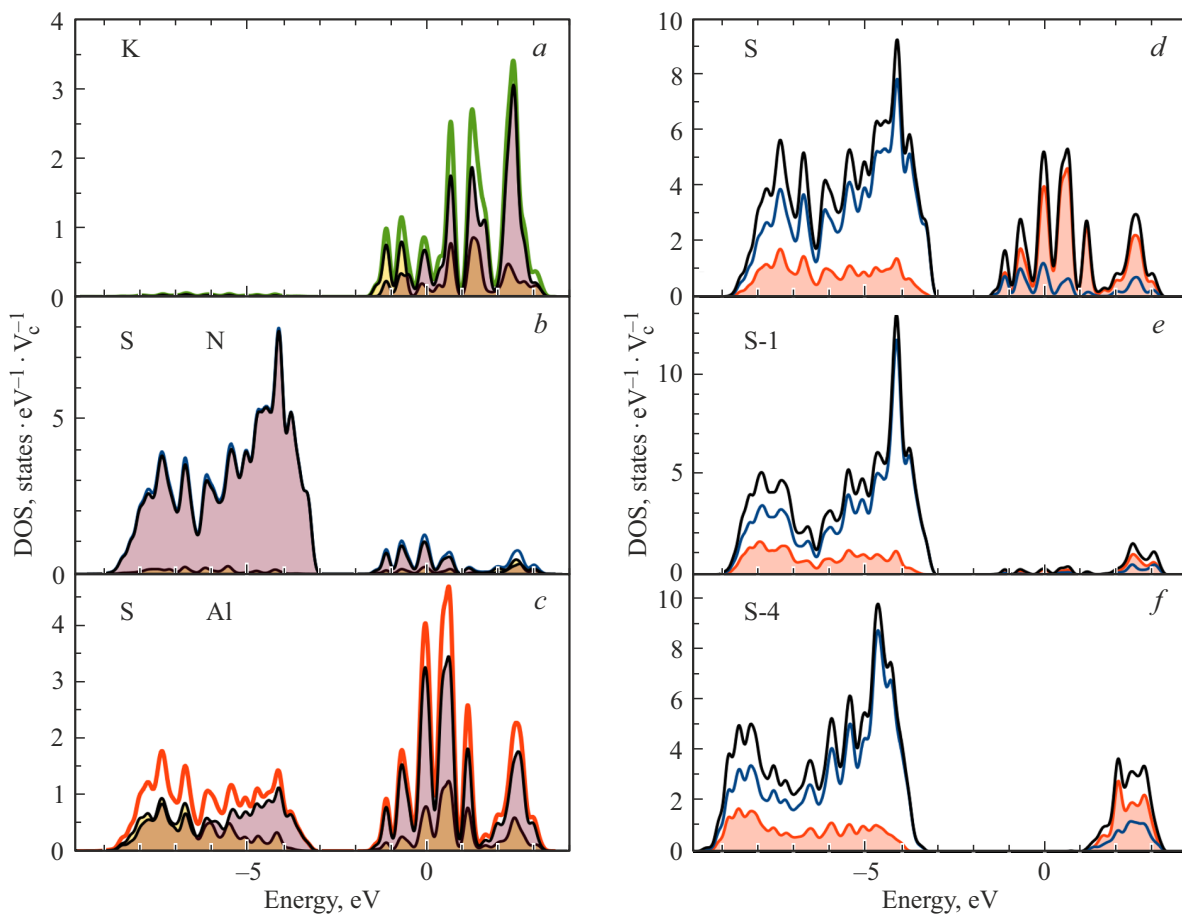


**Figure 3.** Calculated total and partial densities of states of the 2D layer AlN(0001) in the case of adsorption of 0.25 monolayer of K over the N atom. Total and partial densities of states K (a): total density of states — green color and partial densities of states: K 4s — yellow fill, K 4p — pink fill. Partial densities of states N(b) and Al (c) for the surface (S) bilayer AlN. Total and partial densities of states for S (d), S-1 (e) and S-4 (f) bilayers AlN.  $V_c$  — unit cell volume. Total density of states — black, N — blue, N 2s — yellow with fill. Partial densities of states: N 2p — pink color with fill, Al — red color, Al 3p — pink fill and Al 3s — yellow fill.

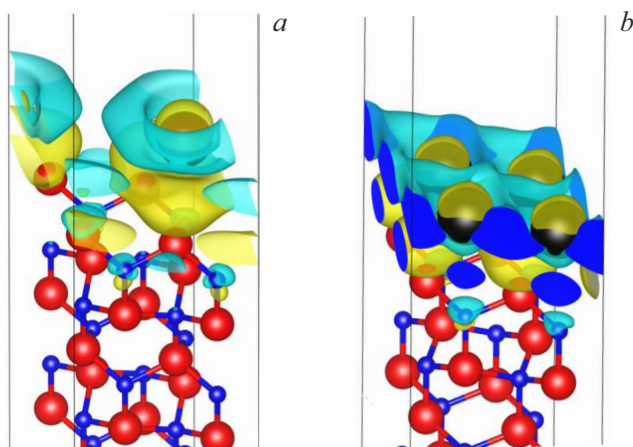


**Figure 4.** The difference in charge density  $\Delta\rho(r)$  after potassium adsorption at a position above a nitrogen atom to cover 0.25 potassium monolayer (a) and a potassium monolayer (b). The areas of depletion of charge density are shown in blue, the areas of accumulation of charge density are shown in yellow. Nitrogen atoms — blue balls, aluminum atoms — red balls, potassium atoms — black balls. The blue color shows the slice  $\Delta\rho(r)$  at the border of the unit cell.

atom and four aluminum atoms. There are also small changes  $\Delta\rho(r)$  near the nitrogen atoms in the surface bilayer. A similar result was obtained when calculating the adsorption of Li on h-AlN [15].

The results of calculating the electronic structure of the K/AlN(0001) system when coating a single potassium monolayer during adsorption of K over N atoms are shown in Figure 5. Figure 5, a shows the zone of surface states of potassium, which is formed by 4s- and 4p-states. The electron density in the adsorbed potassium layer increases, and the electron density shifts towards lower energies, which leads to an increase in the electron density below  $E_F$ . The peaks of the surface states shift towards lower energies:  $-1.76$  eV,  $-1.16$  eV and  $-0.52$  eV. The adsorption bond is formed due to the interaction of sodium valence electrons with unpaired electrons of dangling Al bonds. This interaction leads to a significant change in the electronic structure of the surface bilayer S and in the bilayer S-1, as shown in Figure 5, b, e.

The effect of the adsorbed potassium monolayer also becomes significant for the S-4 bilayer (Figure 5, f). A shift

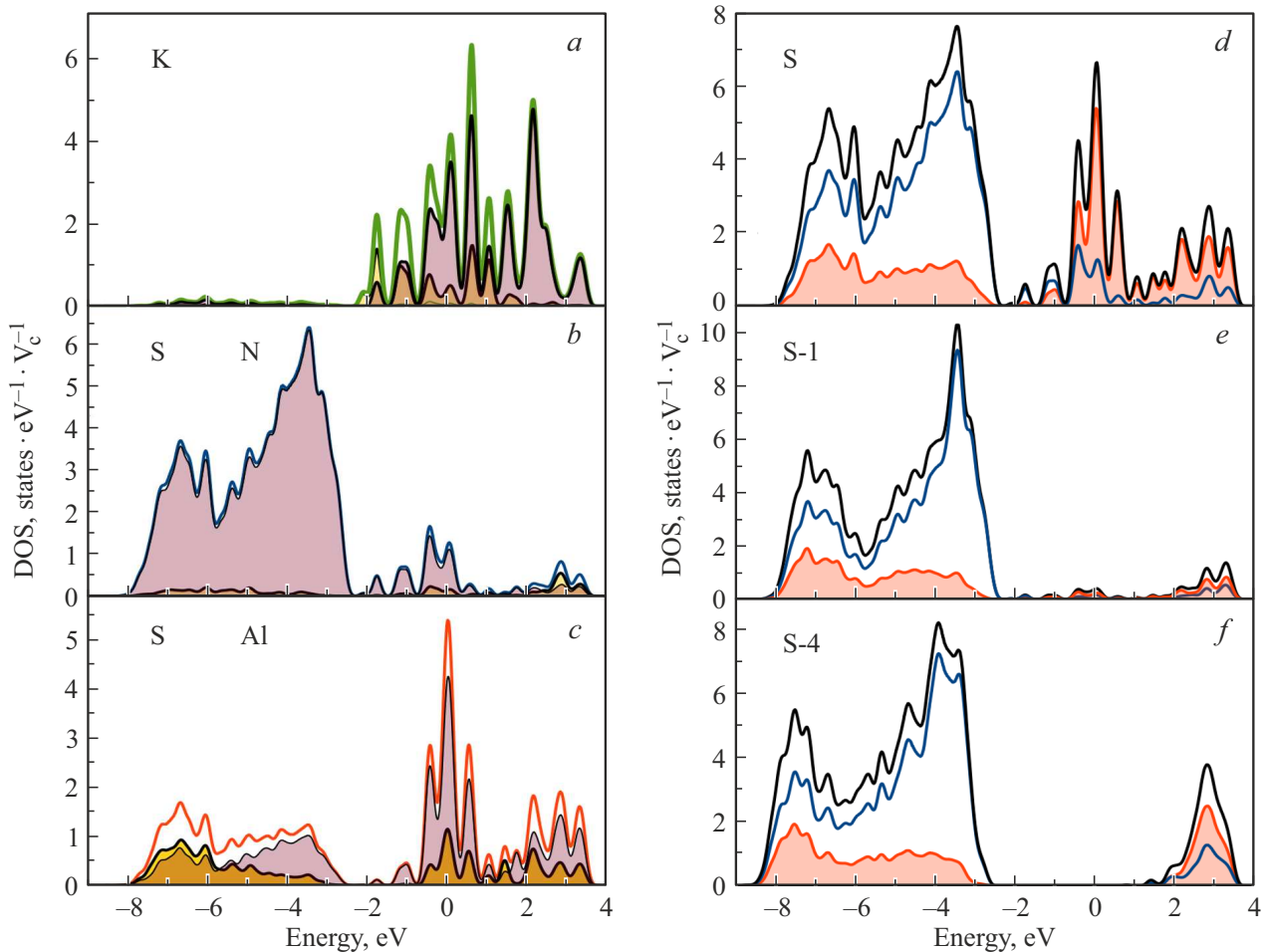


**Figure 5.** Calculated total and partial densities of states of the 2D AlN(0001) layer in the case of adsorption of a monolayer of K over an atom of N. Total and partial densities of states K (a): total density of states — golden color, partial densities of states: K 4s — yellow fill and K 4p — pink fill. Partial densities of states N (b) and Al (c) for the surface (S) bilayer AlN. Total and partial densities of states for S (d), S-1 (e) and S-4 (f) bilayers AlN.  $V_c$  — unit cell volume. Total density of states — black color and partial densities of states: N — blue, N 2s — yellow with fill, N 2p — pink with fill, Al — red, Al 3p — pink fill and Al 3s — yellow fill.

occurs towards lower energies up to 0.65 eV in the region of the surface states of the substrate: the maxima are located at  $-1.77$  eV,  $-1.13$  eV and  $-0.42$  eV. The area of unoccupied states varies slightly. The valence band shifts towards higher energies by 0.65 eV. The width of the pseudo-gap in the S bilayer decreases to zero after adsorption of the monolayer of potassium atoms.

The surface states also shift below the Fermi level in the S-1 bilayer, and the peaks are located at almost the same values as in the S bilayer. The area of unoccupied states varies slightly. The valence band shifts towards higher energies by 0.65 eV. Accordingly, the pseudo-gap on the surface decreases to almost zero values. The electronic structure of the S-4 bilayer is also undergoing changes: the valence band shifts towards high energies by 0.65 eV and the band gap becomes 2.0 eV. Consequently, the adsorption of a monolayer of potassium atoms leads to significant changes in the electronic structure of the 2D AlN layer to a relatively large depth from the surface.

As can be seen from Figure 4, b, the charge accumulates under the potassium atom and the charge leaves the region of the potassium atom, which indicates the formation of a bond between potassium atoms and four aluminum atoms. There are also small changes  $\Delta\rho(r)$  near the nitrogen atoms in the surface bilayer of AlN.

The deposition of a monolayer of potassium atoms strongly changes the electronic structure between the Fermi level and the maximum of the valence band in the near-surface layers of AlN(0001), which makes it possible to change the electronic properties of the surface of AlN.

In the present calculation, the zone of surface states of AlN at the Fermi level changes little during the adsorption of the potassium monolayer, in contrast to the results on the isolation of the zone of surface states in Refs. [16,17]. A zone of induced surface states of potassium was identified in Refs. [16,17] with a maximum of 6.6 eV below  $E_{VBM}$ . It should be noted that the contribution to the region of valence states in the potassium layer is insignificant in the

calculation case (Figure 5, a). The differences between the calculations and experimental data may be due to the fact that the actual topography and stoichiometry of the AlN surface differs from the ideal one for which the present calculation was made. The presence of various surface defects on a real surface can have an impact on the experimental data obtained. The experimental results may also be influenced by the surface cleaning technique.

## 4. Conclusions

The adsorption of potassium atoms in two coatings has been calculated for the first time: 0.25 ML and 1.0 ML on the surface of the 2D layer AlN(0001) by the density functional method. It is shown that when potassium is coated with 0.25 ML, the adsorption energy is almost the same for different adsorption sites: in the dimpled position and above the surface atom of Al or N. The adsorption energy ranges from  $-1.42$  eV to  $-1.53$  eV. The distance between the potassium atom and the layer of Al atoms is 3.08 Å. The adsorption of potassium atoms leads to a shift in the zone of surface states to lower energies. A zone of surface states of potassium below the Fermi level is also formed. In a monolayer coverage, potassium atoms are adsorbed over nitrogen atoms in the surface bilayer of AlN. The adsorption energy of K atoms is  $-0.93$  eV. The adsorption of potassium atoms leads to a further decrease in the energy of the surface states of AlN and potassium. The adsorption of potassium atoms leads to the accumulation of charge density over the surface atoms of Al, which indicates the formation of a bond due to the interaction of valence electrons of potassium with unpaired electrons of Al. The actual topography and stoichiometry of the AlN surface differs from the ideal surface for which the present calculation was made, which led to a discrepancy between the experimental data and the calculation.

## Conflict of interest

The author declares that he has no conflict of interest.

## References

- [1] H. Yang, J. Sun, H. Wang, H. Li, B. Yang. *J. Alloys and Compounds*, **989**, 174330 (2024). DOI: 10.1016/j.jallcom.2024.17433.
- [2] R. Yu, G. Liu, G. Wang, C. Chen, M. Xu, H. Zhou, T. Wang, J. Yu, G. Zhaof, L. Zhang. *J. Mater. Chem. C* **9**, 6, 1852 (2021). DOI: 10.1039/d0tc04182c
- [3] N. Li, C.P. Ho, S. Zhu, Y.H. Fu, Y. Zhu, L. Yao, T. Lee. *Nanophotonics* **10**, 9, 2347 (2021). DOI: 10.1515/nanoph-2021-0130
- [4] S.D.T. Haider, M.A. Shah,, D.-G. Lee, S. Hur. *IEEE Acess* **11**, 58779 (2023). DOI: 10.1109/ACCESS.2023.3276716
- [5] W. Fang, Q. Li, J. Li, Y. Li, Q. Zhang, R. Chen, M. Wang, F. Yun, T. Wang. *Crystals*, **13**, 6, 915 (2023). DOI: 10.3390/cryst13060915
- [6] S. Hagedorn, S. Walde, A. Knauer, N. Susilo, D. Pacak, L. Cancellara, C. Netzel, A. Mogilatenko, C. Hartmann, T. Wernicke, M. Kneissl, M. Weyers. *Phys. Status Solidi A* **217**, 1901022 (2020). DOI: 10.1002/pssa.201901022
- [7] G. Wang, H. Yuan, A. Kuang, W. Hu, G. Zhang, H. Chen. *Int. J. hydrogen energy* **39**, 8, 3780 (2014). DOI: 10.1016/j.ijhydene.2013.12.13
- [8] Y.S. Wang, P.F. Yuan, M. Li, Q. Sun, Y. Jia. *Chin. Phys. Lett.* **28**, 11, 116801 (2011) DOI: 10.1088/0256-307X/28/11/116801
- [9] P. Weichi, L. Haiyang, Z. Xuejing, Z. Wenming, S. Ebrahimi. *Phys. Lett. A* **384**, 18, 126396 (2020). DOI: 10.1016/j.physleta.2020.126396
- [10] V.M. Bermudez. *Surf. Sci. Rep.* **72**, 4, 147 (2017). DOI: 10.1016/j.surfrept.2017.05.001
- [11] L. Liu, Y. Diao. *Mater. Sci. Semicond. Processing* **132**, 105899 (2021). DOI: doi.org/10.1016/j.mssp.2021.105899
- [12] A. Sengupta. *Appl. Surf. Sci.* **451**, 141 (2018). DOI: 10.1016/j.apsusc.2018.04.264
- [13] H. Anaraki-Ardakani. *Phys. Lett. A* **381**, 11, 1041 (2017). DOI: 10.1016/j.physleta.2017.01.010
- [14] S. Sarikurt. *Eskişehir Techn. Univer. J. Sci. Technol. A — Appl. Sci. Eng.* **2019**, **20**, 4, 436 (2019). DOI: 10.18038/estubtda.513854
- [15] S. Munsif, K. Ayub. *J. Molec. Liq.* **259**, 249 (2018). DOI: 10.1016/j.molliq.2018.03.009
- [16] S.N. Timoshnev, G.V. Benemanskaya. *Phys. Complex Syst.* **3**, 1, 21 (2022). DOI: 10.21883/SC.2022.06.53534.9821a
- [17] G.V. Benemanskaya, S.N. Timoshnev, G.N. Iluridze, T.A. Minashvili. *Semicond.* **56**, 6, 387 (2022). DOI: 10.33910/2687-153X-2022-3-1-21-24
- [18] P. Giannozzi, S. Baroni, N. Bonini, M. Calandra, R. Car, C. Cavazzoni, D. Ceresoli, G.L. Chiarotti, M. Cococcioni, I. Dabo, A.D. Corso, S. de Gironcoli, S. Fabris, G. Fratesi, R. Gebauer, U. Gerstmann, C. Gougaussis, A. Kokalj, M. Lazzari, L. Martin-Samos, N. Marzari, F. Mauri, R. Mazzarello, S. Paolini, A. Pasquarello, L. Paulatto, C. Sbraccia, S. Scandolo, G. Sclauzero, A.P. Seitsonen, A. Smogunov, P. Umari, R.M. Wentzcovitch. *J. Phys.: Condens. Matter* **21**, 39, 395502 (2009). DOI: 10.1088/0953-8984/21/39/395502
- [19] J.P. Perdew, A. Zunger. *Phys. Rev. B* **23**, 10, 5048 (1981). DOI: 10.1103/PhysRevB.23.5048.
- [20] V.M. Bermudez, T.M. Jung, K. Doverspike, A.E. Wickenden. *J. Appl. Phys.* **79**, 1, 110 (1996). DOI: 10.1063/1.360917.
- [21] G. Matin, S. Strite, A. Botchkarev, A. Agarwal, A. Rockett, H. Morkoç. *Appl. Phys. Lett.* **65**, 5, 610 (1994). DOI: 10.1063/1.112247

Translated by A.Akhtyamov